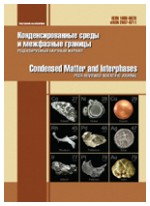

ISSN 1606-867X (Print)
ISSN 2687-0711 (Online)
Condensed Matter and Interphases
Kondensirovannye Sredy i Mezhfaznye Granitsy
https://journals.vsu.ru/kcmf/

Original articles

Research article
https://doi.org/10.17308/kcmf.2026.28/13591

Effect of Sr^{2+} ions on the gas-sensitive properties of $LaCrO_3$ and $GdCrO_3$

Ya. M. Nemykh[1]✉, V. F. Kostryukov[1], I. N. Gorbunov[1], E. V. Tomina[1,2]

[1]*Voronezh State University,*
1, Universitetskaya pl., Voronezh 394018, Russian Federation

[2]*Voronezh State Forestry University*
8, Timiryazeva st., Voronezh 394087, Russian Federation

Abstract

Objectives: Thin films obtained from $La_{1-x}Sr_xCrO_{3-\delta}$ and $Gd_{1-x}Sr_xCrO_{3-\delta}$ (x = 0.05, 0.10, and 0.15) synthesized by the modified citrate method were studied.

Experimental: An analysis of the phase composition, structure, and gas-sensitive properties of films in the presence of carbon monoxide was carried out. Doping with Sr^{2+} ions led to an increase in the defect rate of nanoparticles due to the formation of vacancies in the oxygen sublattice. This phenomenon had a positive effect on their gas-sensitive properties.

Conclusions: It was found that samples of $La_{0.9}Sr_{0.1}CrO_{3-\delta}$ and $Gd_{0.9}Sr_{0.1}CrO_{3-\delta}$ showed the highest sensory response at 180°C, 2.26 and 1.78, respectively. The results obtained confirmed the prospects of using these materials as gas sensors.

Keywords: Nanopowders, Perovskites, Gas-sensitive properties, Pechini method, $LaCrO_3$, $GdCrO_3$, Sr^{2+} doping

Acknowledgements: The research results were partially obtained on the equipment of the Voronezh State University Center for Collective Use: http://ckp.vsu.ru

For citation: Nemykh Y. M., Kostrukov V. F., Gorbunov I. N., Tomina E. V Effect of Sr^{2+} ions on the gas-sensitive properties of $LaCrO_3$ and $GdCrO_3$. *Condensed Matter and Interphases*. 2026;28(1): 81–91. https://doi.org/10.17308/kcmf.2026.28/13591

Для цитирования: Немых Я. М., Кострюков В. Ф., Горбунов И. Н., Томина Е. В. Влияние ионов Sr^{2+} на газочувствительные свойства $LaCrO_3$ и $GdCrO_3$. *Конденсированные среды и межфазные границы*. 2026;28(1): 81–91. https://doi.org/10.17308/kcmf.2026.28/13591

✉ Yaromir M. Nemykh, e-mail: yaromir0202@gmail.com

1. Introduction

Since the 1980s, gas sensors based on metal oxides, such as SnO_2, which are widely used in industry, have been actively studied. However, traditional metal oxide sensors are not able to cover the entire range of tasks of modern industry, which encourages the search for new materials [2]. One of the categories of such materials is compounds with a perovskite structure. Gas-sensitive materials with a perovskite structure have several advantages over binary oxides: high sensitivity, selectivity, and sensor signal values. Synthesis can be carried out at relatively low temperatures. Their gas-sensitive properties can be quite easily and widely controlled, changing both the composition of the material itself, and the nature and concentration of the dopant. In this case, doping can be carried out in two positions, and not in one as with simple oxides. This feature of perovskite-like compounds allows them to contain cationic and oxygen vacancies [3], endowing these compounds with variable electrical and redox properties, which have a decisive influence on gas-sensitive properties [4]. Doping allows you to change the electrical and sensory characteristics of the material, making it more selective.

Perovskite-based gas sensors provide reliable detection of harmful gases in the environment. Such sensors can operate in a wide temperature range and demonstrate selectivity to various gases, such as CO, NH_3, NO_2, etc. At the same time, the maximum values of the sensor signal are observed at lower temperatures. The reduction in comparison with tin and zinc oxides is up to 100°C. These materials are promising for creating sensors with low power consumption. The main mechanisms of sensitivity are chemisorption and catalytic processes occurring on the surface of oxide materials [5, 6].

There are various types of gas sensors based on perovskite-like materials, such as ferrites, cobaltites, stannites, manganites, and other complex oxides.

Ferrites are oxide compounds with the general formula $AFeO_3$, where A is a rare earth element. They show high sensitivity to various gases, especially hydrocarbons and CO. Among ferrites, the most interesting are $LaFeO_3$ and $YFeO_3$, which are successfully used in the detection of liquefied petroleum gases [7].

Cobaltites, such as $LaCoO_3$, have a high catalytic activity and are sensitive to alcohols, CO, and H_2. Doping with oxides such as ZnO improves their sensor characteristics, reducing the detection operating temperature. Due to their high thermal stability, cobaltites are promising materials for use in gas-sensitive sensors operating at elevated temperatures [8].

Stannites, represented by $BaSnO_3$ and $ZnSnO_3$ compounds and $ZnSnO_3$, exhibit sensitivity to NO_2 and n-propanol. They have good selectivity and stability, which makes them in demand for monitoring industrial emissions and indoor air quality. The high operating temperature of stannite-based sensors (up to 900°C) limits their use, but active research is aimed at reducing these temperatures by modifying the structure and morphology of the material [9, 10].

Manganites such as $YMnO_3$ show increased sensitivity to hydrogen sulfide (H_2S) and ammonia (NH_3). They have a stable structure and can operate at relatively low temperatures (about 100°C). Studies show that varying the composition of manganites makes it possible to control their sensory characteristics, which opens up prospects for their application in environmental monitoring and industrial safety [11].

Another promising group of materials is chromites of rare-earth elements, for example, $LaCrO_3$ [12] and $GdCrO_3$, which are studied in our laboratory [13]. They demonstrate resistance to high temperatures, which makes them promising for sensor applications. An analysis of the literature shows that doping of chromites can change their electronic and surface properties. In [14], a wide range of possibilities for modifying $LaCrO_3$ to change its physical properties was demonstrated, and in [15], the authors found that the mechanism of electrical conductivity $GdCrO_3$ is described by the Mott model of hopping conductivity with a variable hop length.

Thus, the aim of this work is to study the gas-sensitive properties of lanthanum and gadolinium chromites doped with Sr^{2+} ions. The synthesis and complex analysis of the

composition, structure, and sensory response of $La_{1-x}Sr_xCrO_{3-\delta}$ and $Gd_{1-x}Sr_xCrO_{3-\delta}$ (x = 0.05, 0.10, and 0.15) to the presence of carbon monoxide in the atmosphere was performed. The choice of strontium ion concentrations is determined, on the one hand, by the need for a sufficiently significant impact on the target characteristics, and, on the other hand, by the need to form a single-phase material.

2. Experimental

Nanopowders $Ls_{1-x}Sr_xCrO_{3-\delta}$ and $Gd_{1-x}Sr_xCrO_{3-\delta}$ (x = 0.05, 0.10, and 0.15) were synthesized by the modified citrate method [16]. This method is based on the complexation of cations with citric acid, followed by thermal decomposition. Lanthanum, gadolinium, strontium, and chromium nitrates, citric acid, and ammonium hydroxide were used as starting materials

First, the calculated amounts of nitrates of $La(NO_3)_3 \cdot 6H_2O$ (or $Gd(NO_3)_3 \cdot 6H_2O$), $Sr(NO_3)_2 \cdot 4H_2O$, and $Cr(NO_3)_3 \cdot 9H_2O$ were dissolved in distilled water with constant stirring. The resulting solution was boiled to form a sol, after which an ammonia solution was added dropwise until pH 7–8 was established. During the deposition, a gel was formed. The resulting gel was cooled to room temperature, after which, with constant stirring, citric acid was added to the system in a stoichiometric ratio of 3:1 with respect to the number of metal cations.

The solution was heated until the water completely evaporated and a gel-like precipitate was formed. The resulting gel was calcined at 300–350°C to remove organic compounds. The final formation of nanopowders was achieved by heat treatment in a muffle furnace at 700°C for 4 hours.

The resulting nanopowders were dispersed in ethyl alcohol with the addition of cetyltrimethylammonium bromide (CTAB) as a surfactant to form a paste, and then they were applied to a conductive element (silicon wafer) by spin-coating (SpinNXG-P1H installation) and annealed for 1 hour at a temperature of 100°C. The deposition mode (first 1 minute - 2000 rpm, then 20 minutes - 5000 rpm) was determined by calibration dependences and provided a fixed thickness of 150±7 nm [17, 18].

3. Study of composition and structure

X-ray phase analysis

The study of the phase compositions of $La_{1-x}Sr_xCrO_{3-\delta}$ and $Gd_{1-x}Sr_xCrO_{3-\delta}$ (x = 0.05, 0.10, and 0.15) was performed on a Thermo ARL X'TRA X-ray diffractometer (CuK_α radiation, λ = 1.5418 Å). When examining the X-ray diffraction patterns of the obtained samples (Fig. 1), it was found that all peaks in the graphs of the intensity dependence on the angle 2θ correspond to the perovskite structure, which is confirmed by comparison with the bases of X-ray diffractograms [19].

A detailed examination of the diffractograms shows a shift in the peaks of the doped samples (Tables 1, 2) relative to the undoped ones, which indicates a change in the lattice parameters due to strontium ions embedded in it.

The upward shift of the peaks of doped lanthanum chromite was about 0.06, 0.03, and 0.04 deg. for 5 at. %, 10 at. % and 15 at. % strontium, respectively. This is explained by the fact that the ionic radius of Sr (1.16 Å) is smaller than the ionic radius of La (1.50 Å), which leads to compression of the crystal lattice [20].

The lower shift of the peaks of doped gadolinium chromite were about 0.02, 0.03, and 0.03 deg. for 5 at. %, 10 at. % and 15 at. % strontium, respectively. This is explained by the fact that the ionic radius of Sr (1.16 Å) is larger than the ionic radius of Gd (0.98 Å), which leads to an increase in interplanar distances [20].

Based on the obtained data, the volume of unit cells of the synthesized samples was calculated in the absence and presence of doping. For unsubstituted lanthanum chromite, the unit cell volume was 234.34 $(Å)^3$, and for gadolinium chromite it was 222.95 $(Å)^3$. The tabulated values were 234, 46, and 223.71 $(Å)^3$, respectively (calculated on the basis of data from [19]). Doping with strontium ions led to a change in the unit cell volume. Lanthanum chromite doped with 10 at. % Sr the unit cell volume was 233.74 $(Å)^3$, while gadolinium chromite doped with 10 at. % Sr it was 223.57 $(Å)^3$. The results obtained, on the one hand, are in good agreement with the tabulated values, and, on the other hand, showed a regular change in the volume of unit cells when the initial cations were replaced during doping with a cation

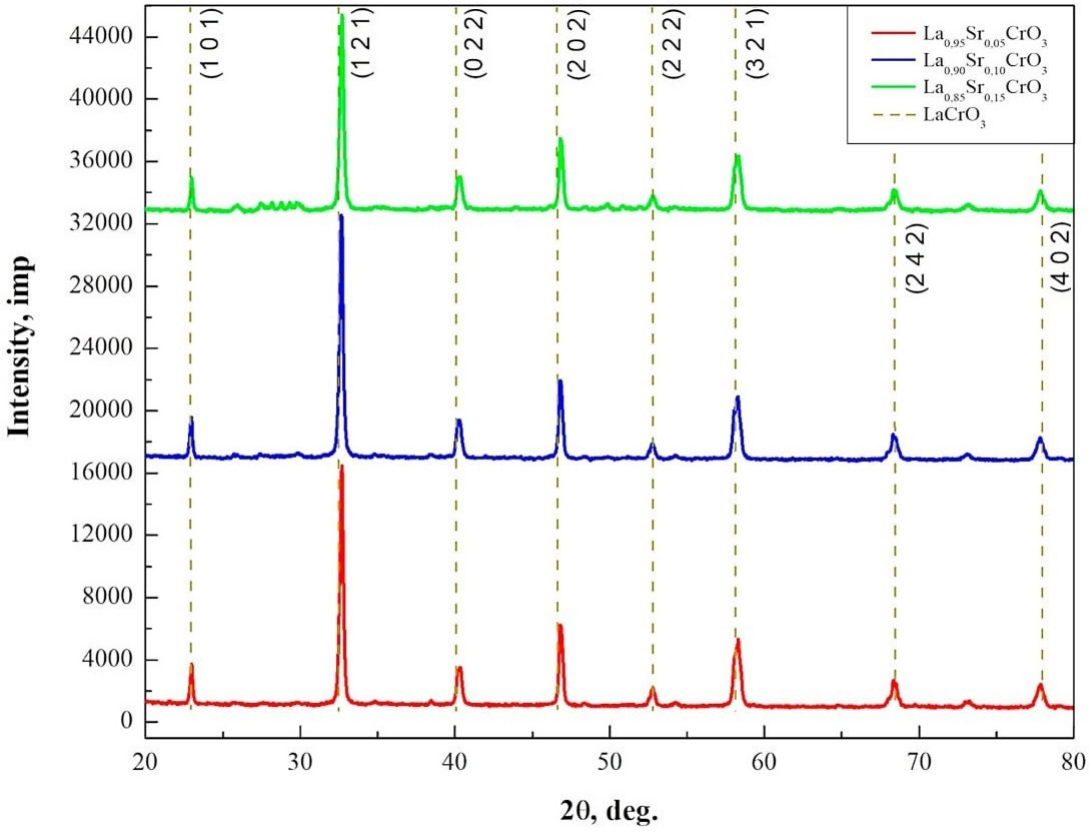

a

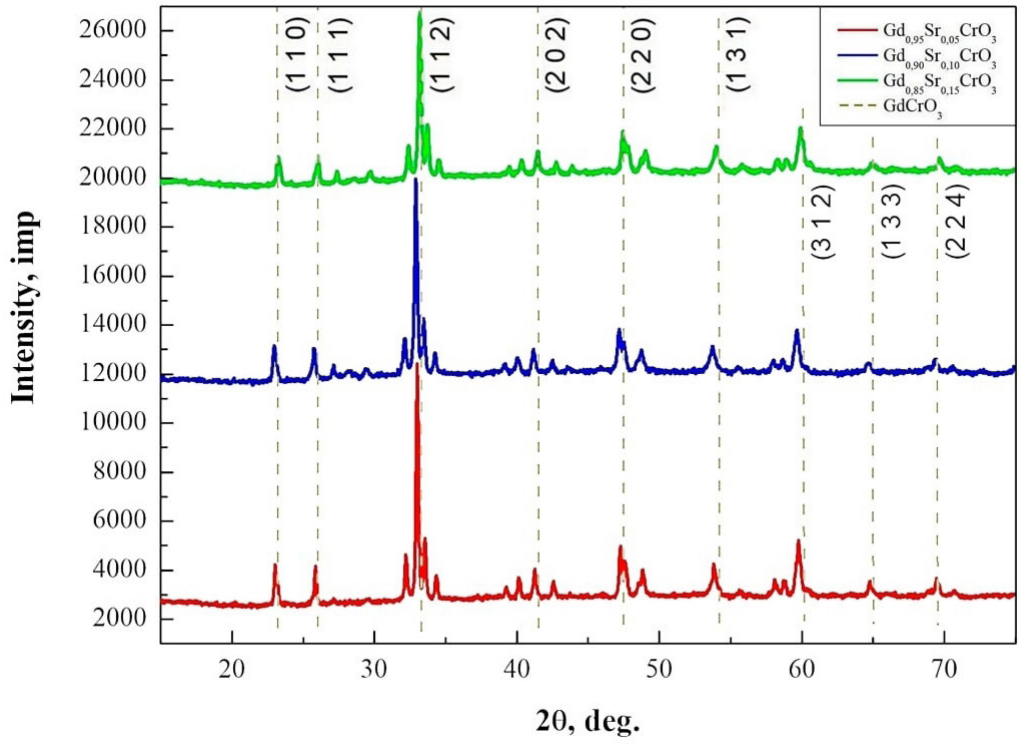

b

Fig. 1. Comparison of X-ray diffractograms of doped $La_{1-x}Sr_xCrO_{3-\delta}$ (a) and $Gd_{1-x}Sr_xCrO_{3-\delta}$ (b) nanopowders with individual samples

Table 1. 2θ value for a series of $La_{1-x}Sr_xCrO_{3-\delta}$ samples (x = 0.05, 0.10, and 0.15) relative to unsubstituted $LaCrO_3$

Sample	Value 2θ for unsubstituted sample / value 2θ for doped sample							
	(101)	(121)	(022)	(202)	(222)	(321)	(242)	(402)
$La_{0.95}Sr_{0.05}CrO_{3-\delta}$	22.90 / 22.96	32.60 / 32.72	40.12 / 40.10	46.76 / 46.82	52.68 / 52.72	58.26 / 58.32	68.30 / 68.36	77.72 / 77.82
$La_{0.9}Sr_{0.1}CrO_{3-\delta}$	22.90 / 22.92	32.60 / 32.64	40.12 / 40.14	46.76 / 46.80	52.68 / 52.72	58.26 / 58.28	68.30 / 68.32	77.72 / 77.76
$La_{0.85}Sr_{0.15}CrO_{3-\delta}$	22.90 / 22.96	32.60 / 32.66	40.12 / 40.16	46.76 / 46.82	52.68 / 52.74	58.26 / 58.24	68.30 / 68.34	77.72 / 77.80

Table 2. 2θ value for a series of $Gd_{1-x}Sr_xCrO_{3-\delta}$ samples (x = 0.05, 0.10, and 0.15) relative to unsubstituted $GdCrO_3$

Sample	Value 2θ for unsubstituted sample / value 2θ for doped sample							
	(110)	(111)	(112)	(202)	(220)	(131)	(312)	(133)
$Gd_{0.95}Sr_{0.05}CrO_{3-\delta}$	23.24 / 23.26	26.04 / 26.02	33.20 / 33.16	41.46 / 41.42	47.46 / 47.44	54.00 / 53.98	59.92 / 59.92	64.98 / 64.96
$Gd_{0.9}Sr_{0.1}CrO_{3-\delta}$	23.24 / 23.26	26.04 / 26.02	33.20 / 33.16	41.46 / 41.42	47.46 / 47.42	54.00 / 53.94	59.92 / 59.88	64.98 / 64.90
$Gd_{0.85}Sr_{0.15}CrO_{3-\delta}$	23.24 / 23.26	26.04 / 26.02	33.20 / 33.16	41.46 / 41.42	47.46 / 47.42	54.00 / 53.96	59.92 / 59.88	64.98 / 64.92

of a smaller (in the first case) and larger (in the second case) radius.

Local X-ray spectral microanalysis

The elemental composition of the powders was analyzed using a JEOL-6510LV scanning electron microscope with a Bruker energy dispersive microanalysis system. The results of the study are presented in Tables 3 and 4. This method is not able to estimate the oxygen content [21], so only the cation content is presented in the analysis results. In addition to the direct experimental data, Tables 3 and 4 add a column that shows the ratio of cations in the samples and characterizes the proximity of the composition of the obtained samples to the one specified during synthesis.

Both series of samples showed a fairly close correspondence to the required stoichiometric

Table 3. Result of elemental composition analysis of unsubstituted lanthanum chromite and strontium-doped lanthanum chromite nanopowders

Nominal composition of samples	Elemental composition, at. %			
	La	Sr	Cr	[Sr]/([Sr]+[La])
$LaCrO_3$	19.4	–	20.6	–
$La_{0.95}Sr_{0.05}CrO_{3-\delta}$	19.54	0.99	20.61	0.48
$La_{0.9}Sr_{0.1}CrO_{3-\delta}$	18.92	1.98	20.66	0.95
$La_{0.85}Sr_{0.15}CrO_{3-\delta}$	18.03	3.02	20.73	0.14

Table 4. Result of elemental composition analysis of unsubstituted gadolinium chromite and strontium-doped gadolinium chromite nanopowders

Nominal composition of samples	Elemental composition, at. %			
	Gd	Sr	Cr	[Sr]/([Sr]+[Gd])
$GdCrO_3$	23.9	–	24.2	–
$Gd_{0.95}Sr_{0.05}CrO_{3-\delta}$	19.42	0.91	21.06	0.045
$Gd_{0.9}Sr_{0.1}CrO_{3-\delta}$	19.03	1.86	21.03	0.089
$Gd_{0.85}Sr_{0.15}CrO_{3-\delta}$	18.23	2.89	21.22	0.137

ratio. At the same time, according to the results of the Local X-ray spectral microanalysis, it was found that in the $La_{1-x}Sr_xCrO_{3-\delta}$ system (x = 0.05, 0.10, and 0.15), strontium was embedded in a larger amount, which is associated with a simpler substitution of a large La^{3+} ion (ionic radius 1.50 Å) with a Sr^{2+} ion (ionic radius 1.04 Å) of a smaller size. In the $Gd_{1-x}Sr_xCrO_{3-\delta}$ system (x = 0.05, 0.10, and 0.15), strontium was embedded in a smaller amount, since the ionic radius of Gd is 0.96 Å [20].

At the same time, despite the fact that the oxygen content has not been experimentally determined, it can be assumed that in the synthesized samples there will be a certain lack of oxygen associated with the formation of vacancies in the oxygen sublattice, which arises due to the need to compensate for the positive charge during doping with double-charged strontium cations.

4. Particle size study

Transmission electron microscopy

In this work, the obtained powders were examined using a ZEISS Libra 120 transmission electron microscope. Sample preparation was carried out as follows. 5 ml of distilled water was poured into a glass, 0.15 g of gelatin, 1 mg of the test sample were added and placed on a heated magnetic stirrer. The agitator was used for more uniform distribution of nanoparticles in the prepared suspension. Next, objects were caught using a copper mesh with a carbon replica and inserted into the object holder. The results obtained are shown in Fig.2.

According to the TEM data, the particle size ranged from 25 to 35 nm. The dependence of the particle size during the transition from

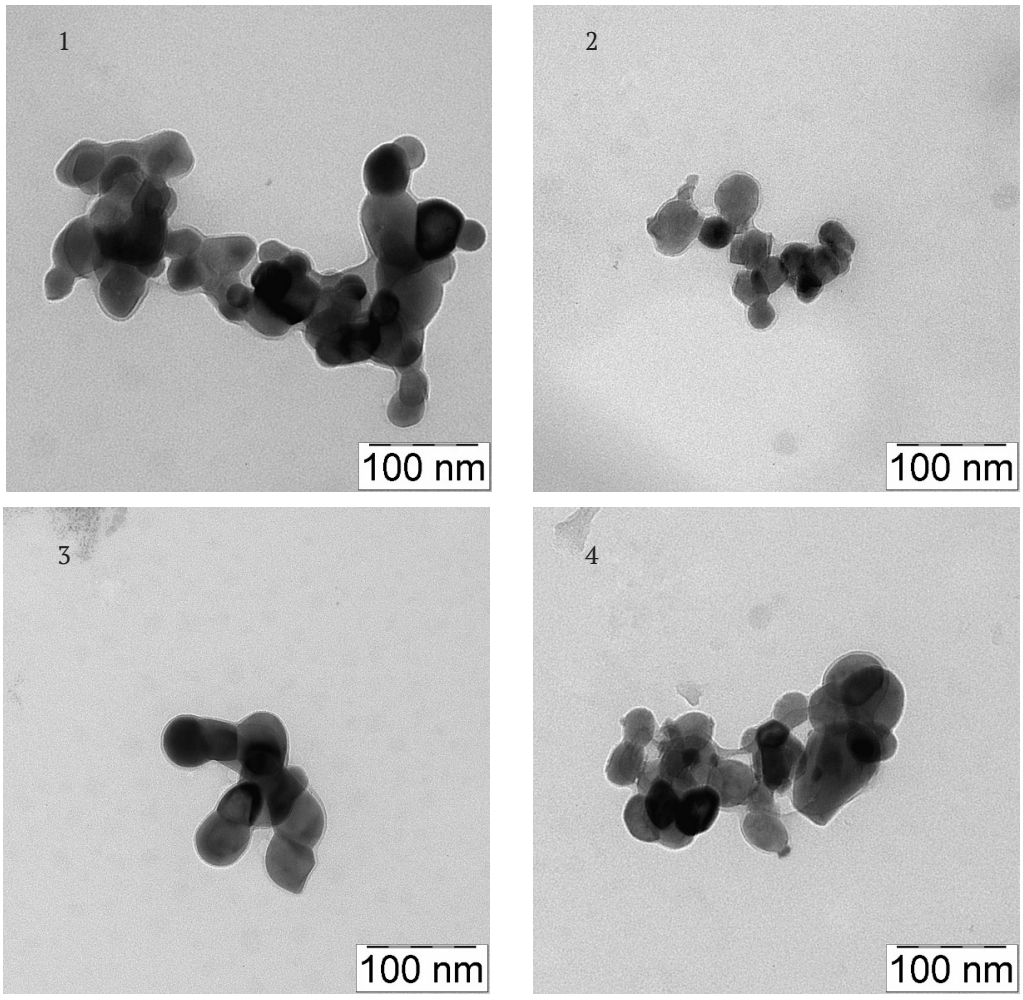

Fig. 2. TEM images of nanoparticles *1* – $LaCrO_3$; *2* – $La_{0,9}Sr_{0,1}CrO_{3-\delta}$; *3* – $GdCrO_{3-\delta}$; *4* – $Gd_{0.9}Sr_{0.1}CrO_{3-\delta}$

unsubstituted to doped chromites has not been established.

5. Investigation of gas-sensitive properties

The specific surface resistance of films made from nanopowders of the $La_{1-x}Sr_xCrO_{3-\delta}$ and $Gd_{1-x}Sr_xCrO_{3-\delta}$ systems (x = 0, 0.05, and 0.1) was measured by the four-probe Van der Pau method. The method was similar to that described in [22, 23]. The studies were performed in air (Fig. 3) and in the presence of carbon monoxide (Fig. 4). Measurements were performed 3 times for each of the samples. The gas concentration was 50 ppm, and the temperature range of the study was 20–400°C. The required carbon monoxide concentration was achieved by diluting the certified gas mixture with dry synthetic air. Measurements were carried out in a stationary system (a closed chamber with a volume of 50 ml). Before each new experiment, the system was purged with synthetic air.

The results of measuring the resistivity of doped samples were compared with the resistivity of unsubstituted $LaCrO_3$ and $GdCrO_3$.

During the measurement process, the analyzed reducing agent gas was adsorbed, during which the free electrons of the adsorbed gas transferred to the sensor surface, increasing the number of mobile charges and reducing the temperature of the onset of a sharp change in resistance.

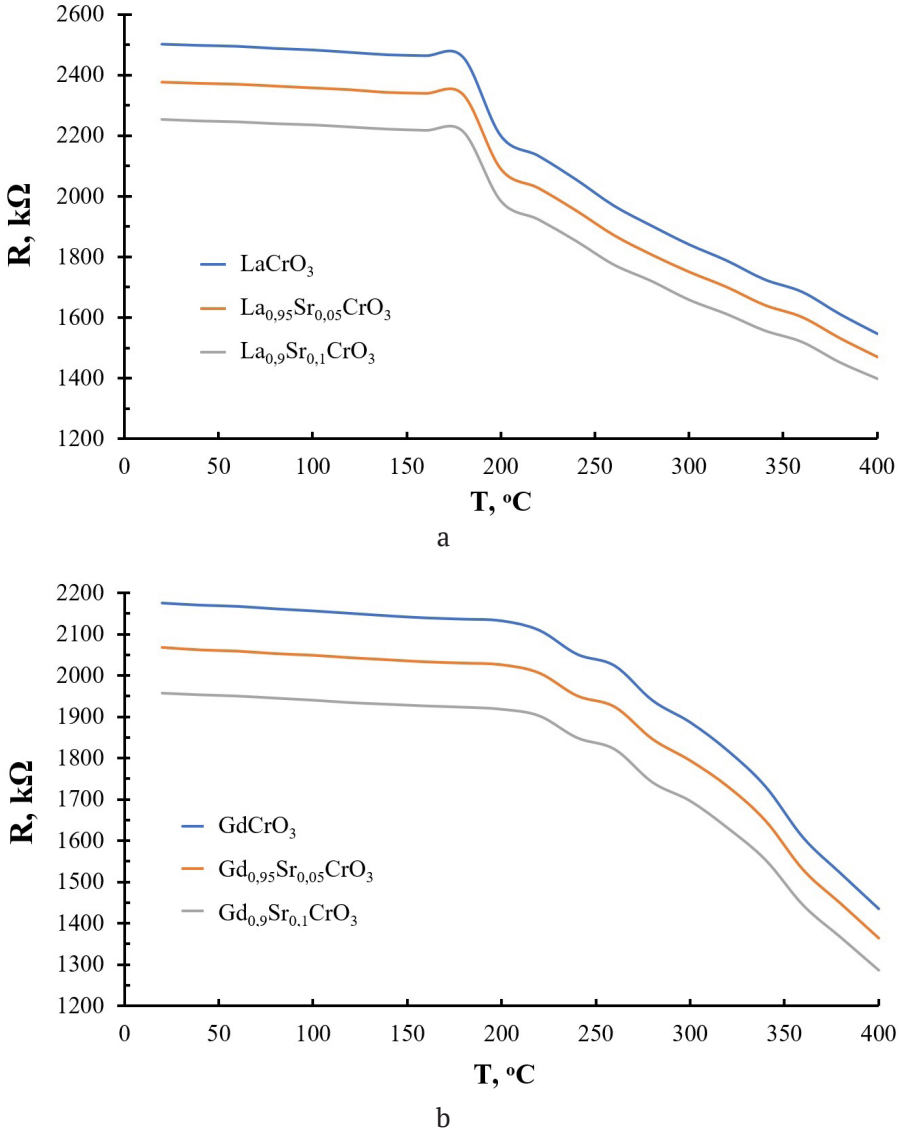

Fig. 3. Dependence of the resistivity of thin films of $La_{1-x}Sr_xCrO_{3-\delta}$ (x = 0, 0.05 and 0.1) (a) and $Gd_{1-x}Sr_xCrO_{3-\delta}$ (x = 0.05 and 0.1)

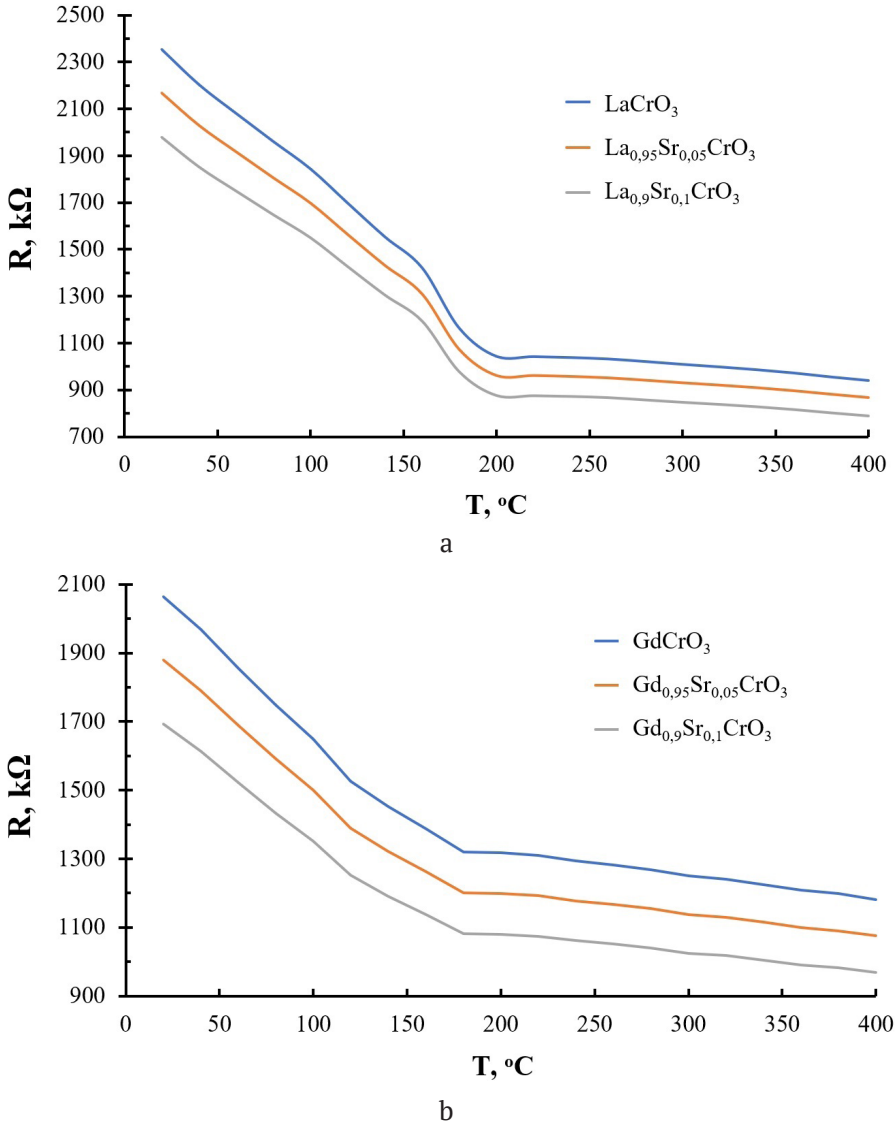

Fig. 4. Dependence of the resistivity of thin films of $La_{1-x}Sr_xCrO_{3-\delta}$ (x = 0, 0.05 and 0.1) (a) and $Gd_{1-x}Sr_xCrO_{3-\delta}$ (x = 0, 0.05 and 0.1) (b) in the presence of carbon monoxide (50 ppm) in the atmosphere

This phenomenon confirms that the resulting chromites are semiconductors.

The introduction of strontium ions into the crystal lattice of lanthanum chromite and gadolinium chromite reduced their resistivity. This is explained by the ionic structure of the crystal: the appearance of uncompensated charges during the substitution of La^{3+} or Gd^{3+} for Sr^{2+} contributed to the formation of oxygen vacancies, which led to a decrease in resistivity, indicating *n*-type conductivity in lanthanum and gadolinium chromites.

According to the results of measuring the resistivity of gadolinium and lanthanum chromites, the resistance of the former is lower. This is explained by the large number of oxygen vacancies in the samples of the $Gd_{1-x}Sr_xCrO_{3-\delta}$ (x = 0, 0.05, and 0.1) system detected by the local X-ray spectral microanalysis.

Based on the obtained values of the resistivity of the samples, the sensory response was calculated using the formula $S_r = R_a/R_g$, where S_r is the gas-sensitive response, R_a is the specific surface resistance of films in air, and R_g is the specific surface resistance of films in the presence of a reducing gas [24]. The dependences of the sensory response on temperature are shown in Fig. 5.

According to the data obtained, lanthanum chromite, unsubstituted and doped with strontium, exhibited the strongest sensory response to carbon

monoxide (CO) at 180°C. Unsubstituted and doped gadolinium chromite at similar temperatures also showed a peak value of the sensory response, but the value of the sensory response was lower than that of the lanthanum chromite samples. A comparison of the sensory responses of doped samples with unsubstituted samples showed that the introduction of strontium into the systems allowed a stronger sensory response, and an increase in the concentration of introduced strontium contributed to a strengthening of the response.

From Fig. 5a it follows that for the $La_{1-x}Sr_xCrO_{3-\delta}$ system (x = 0, 0.05, and 0.1) at 180°C, the sensory responses in the presence of carbon monoxide (50 ppm concentration) were 2.11, 2.18, and 2.26, respectively. The graph itself has a clear maximum, which indicates the accuracy of the gas sensor. For the $Gd_{1-x}Sr_xCrO_{3-\delta}$ (x = 0, 0.05, and 0.1) system (Fig. 5b), the sensory responses under similar conditions were 1.62, 1.69, and 1.78, respectively, which was weaker than the response of lanthanum chromites. The peak graph has similar values at 180 and 200°C.

The high values of sensory response for lanthanum chromites is due to its high resistivity, since during the adsorption of reducing agent gas on the film surface, the number of charge carriers in the system increased, which led to a sharp change in the resistivity.

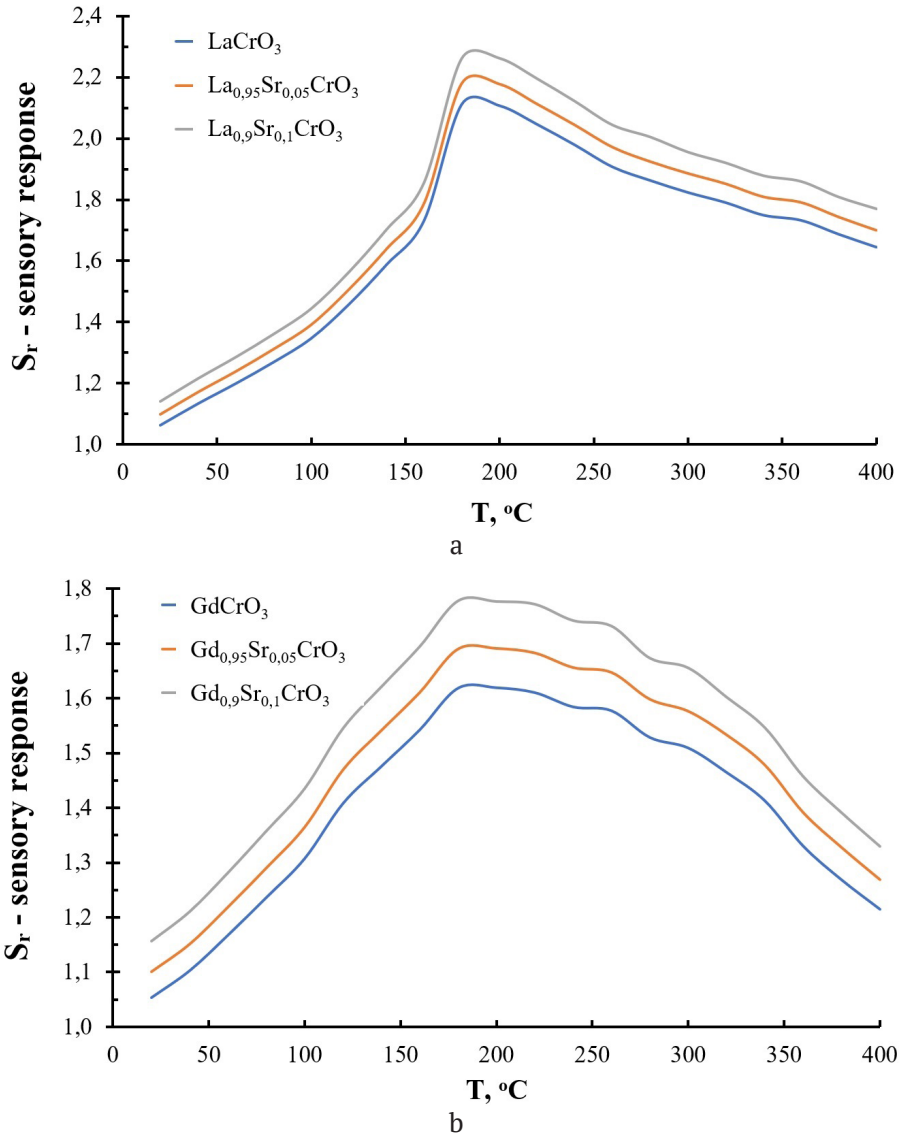

Fig. 5. Temperature dependence of the sensory response to carbon monoxide (50ppm) for thin films of $La_{1-x}Sr_xCrO_{3-\delta}$ (x = 0, 0.05 and 0.1) (a) and $Gd_{1-x}Sr_xCrO_{3-\delta}$ (x = 0, 0.05 and 0.1) (b)

6. Conclusions

Synthesis of $La_{1-x}Sr_xCrO_{3-\delta}$ and $Gd_{1-x}Sr_xCrO_{3-\delta}$ by the Pechini method made it possible to obtain materials with a high degree of uniformity and controlled particle size. The X-ray phase analysis confirmed the presence of a perovskite-like structure of the synthesized compounds and revealed the effect of doping with Sr^{2+} ions on the crystal lattice parameters. Dopant embedding was manifested in a change in interplanar distances associated with the difference in the ionic radii of the substituted element and the dopant. Strontium doping led to an increase in the concentration of oxygen vacancies, which had a positive effect on the sensory characteristics of the materials. Studies of gas-sensitive properties have shown that nanopowders exhibit the maximum response to CO at 180°C. The samples with the highest content of Sr^{2+} ions showed high sensitivity, which is explained by the optimal balance of the defective structure and mobility of charge carriers. The results obtained show the promise of using these nanomaterials for gas sensors.

Author contributions

The authors contributed equally to this article.

Conflict of interests

The authors declare that they have no known competing financial interests or personal relationships that could have influenced the work reported in this paper.

References

1. Anishhik V. M., Konjushko L. I., Jarmolovich V. A., Gorbachevskij D. A., Gerasimova T. G. Structure and properties of tin dioxide films. *Inorganic Materials*. 1995;31(4): 338–341. (in Russ.)

2. Rembeza E. S., Rembeza S. I., Svistova T. V., Dyrda N. N. Methods for improving gas-sensing properties of SnO_2 films for gas sensors. *Izvestija vysshih uchebnyh zavedenij. Jelektronika*. 2006;4: 3–8. (in Russ.). Available at: https://translit.ru/ru/bsi/

3. Kuklja M. M., Mastrikov Y. A., Jansang B., Kotomin E. A. The Intrinsic defects, disordering, and structural stability of $Ba_xSr_{1-x}Co_yFe_{1-y}O_{3-\delta}$ perovskite solid solutions. *The journal of Physical Chemistry C*. 2012;116: 18605–18611. https://doi.org/10.1021/jp304055s

4. Bulemo P. M., Kim I.-D. Recent advances in ABO_3 perovskites: their gas-sensing performance as resistive-type gas sensors. *Journal of the Korean Ceramic Societ*. 2020;57: 24–39. https://doi.org/10.1007/s43207-019-00003-1

5. Fergus J. W. Perovskite oxides for semiconductor-based gas sensors. *Sensors and Actuators B*. 2007;123: 1169–1179. https://doi.org/10.1016/j.snb.2006.10.051

6. Zhu L. Y., Ou L. X., Mao L. W., Wu X.-Y., Liu Y.-P., Lu H. L. Advances in noble metaldecorated metal oxide nanomaterials for chemiresistive gas sensors: Overview. *Nano-Micro Letters*. 2023;15(1). https://doi.org/10.1007/s40820-023-01047-z

7. Avadhesh K. Y., Rajnees K. S., Prabhakar S. Fabrication of lanthanum ferrite based liquefied petroleum gas sensor. *Sensors and Actuators B: Chemical*. 2016;229: 25–30. https://doi.org/10.1016/j.snb.2016.01.066

8. Wenbo Q., Zhenyu Y., Hongliang G., Renze Z., Fanli M. Perovskite-structured $LaCoO_3$ modified ZnO gas sensor and investigation on its gas sensing mechanism by first principle. *Sensors and Actuators: B. Chemical*. 2021;341: 1–15. https://doi.org/10.1016/j.snb.2021.130015

9. Cerda J., Arbiol J., Dezanneau G., Dıaz R., Morante J. R. Perovskite-type $BaSnO_3$ powders for high temperature gas sensor applications. *Sensors and Actuators: B. Chemical*. 2002;84: 21–25. https://doi.org/10.1016/s0925-4005(02)00005-9

10. Yaoyu Y., Yanbai S., Pengfei Z., Rui L., Ang L. Fabrication, characterization and n-propanol sensing properties of perovskite-type $ZnSnO_3$ nanospheres based gas sensor. *Applied Surface Science*. 2020;509: 1–10. https://doi.org/10.1016/j.apsusc.2020.145335

11. Balamurugan C., Lee D. W. Perovskite hexagonal $YMnO_3$ nanopowder as p-type semiconductor gas sensor for H_2S detection. *Sensors and Actuators B: Chemical*. 2015;221: 857–866. https://doi.org/10.1016/j.snb.2015.07.018

12. Prashant B. K., Kailas H. K., Uday G. D., Umesh J. T., Sachin G. S. Fabrication of thin film sensors by spin coating using sol-gel $LaCrO_3$ perovskite material modified with transition metals for sensing environmental pollutants, greenhouse gases and relative humidity. *Environmental Challenges*. 2021;3: 1–13. https://doi.org/10.1016/j.envc.2021.100043

13. Nemykh Ya. M., Kostryukov V. F., Gorbunov I. N. Synthesis of nanopowders of gadolinium chromite and lanthanum chromite with gas-sensitive properties. *Proceedings of Voronezh State University. Series: Chemistry. Biology. Pharmacy*. 2024;3: 13–21. (in Russ.). Available at: https://elibrary.ru/item.asp?id=72799790

14. Duran A., Falconi R., Mata J., Huerta L., Gonzalez M., Reguera E., Torres J. C. From $LaCrO_3$ towards $LaCr_{0,2}Mn_{0,2}Fe_{0,2}Al_{0,2}Ga_{0,2}O_3$ high-entropy ceramic compound: crystal structure, dielectric and magnetic properties. *Journal of the European Ceramic Society*. 2025;45: 1–19. https://doi.org/10.1016/j.jeurceramsoc.2024.116927

15. Javed M., Arif Khan A., Kazmi J., … Mohamed M. A. Variable range hopping transport and dielectric relaxation mechanism in $GdCrO_3$ rare-earth orthochromite perovskite. *Journal of Rare Earths*. 2023;42: 1304–1316. https://doi.org/10.1016/j.jre.2023.07.006

16. Moreno L. C., Valencia J. S., Landínez Téllez D. A., … Fajardo F. Preparation and structural study of $LaMnO_3$ magnetic material. *Magnetism and Magnetic Materials*. 2008;320(14): e19–e21. https://doi.org/10.1016/j.jmmm.2008.02.052

17. Yakimchu M. A., Eliseeva E. S., Kostryukov V. F. Nanocrystalline films based on $YCrO_3$ and $LaCrO_3$ yttrium

and lanthanum chromites doped with strontium ions Sr^{2+} as a basis for semiconductor gas sensors. *Condensed Matter and Interphases*. 2024;26(3): 536–546. https://doi.org/10.17308/kcmf.2024.26/12229

18. Kostryukov V. F., Parshina A. S., Mittova I. Ya. Preparation of gas-sensing thin Sr^{2+}-doped $YFeO_3$ films. *Inorganic Materials*. 2024;60(13): 1482–1490. https://doi.org/10.1134/s0020168525700232

19. JCPDS PCPDFWIN: A Windows-based retrieval and display program for accessing the ICDD PDF-2 database, International Centre for Diffraction Data. 1997.

20. Bugaenko L. T., Ryabykh S. M., Bugaenko A. L. A nearly complete system of average crystallographic ionic radii and its use for determining ionization potentials. *Moscow University Chemistry Bulletin*. 2008;63(6): 303–317. https://doi.org/10.3103/s0027131408060011

21. Krishtal M. M., Jasnikov I. S., Polunin V. I., Filatov A. M., Ul'janenkov A. G. *Scanning electron microscopy and X-ray spectral microanalysis**. Moscow: Tehnosfera Publ.; 2009. 208 p. (in Russ.)

22. *Four-probe method for measuring the electrical resistance of semiconductor materials: a teaching aid for the special practical course "Physics of semiconductor materials and devices" for students of the physics department**. N. A. Poklonskogo (ed.). Minsk: BGU Publ.; 1998. 46 p. (in Russ.)

23. Rembeza S. I., Svistova T. V., Rembeza E. S., Borsyakova O. I. The microstructure and physical properties of thin SnO_2 films. *Semiconductors*. 2001;35(7): 762–765. https://doi.org/10.1134/1.1385709

24. Kostryukov V. F., Parshina A. S., Sladkopevtsev B. V., Mittova I. Ya. Thin films on the surface of GaAs, obtained by chemically stimulated thermal oxidation, as materials for gas sensors. *Coatings (MDPI)*. 2022;12(12): 1819–1828. https://doi.org/10.3390/coatings12121819

** Translated by author of the article*

Information about the authors

Yaromir M. Nemykh, 2st year postgraduate student of the Department of Materials Science and Nanosystems Industry, Voronezh State University (Voronezh, Russian Federation).

https://orcid.org/0009-0009-3189-6018

yaromir0202@gmail.com

Viktor F. Kostryukov, Dr. Sci. (Chem.), Associate Professor at the Department of Materials Science and Industry of Nanosystems, Voronezh State University (Voronezh, Russian Federation).

https://orcid.org/0000-0001-5753-5653

vc@chem.vsu.ru

Ivan N. Gorbunov, 1st year Master's student of the Department of Materials Science and Industry of Nanosystems, Voronezh State University (Voronezh, Russian Federation).

https://orcid.org/0009-0001-5170-7909

wot4114@gmail.com

Elena V. Tomina, Dr. Sci. (Chem.), Head of the Department of Chemistry, Voronezh State Forestry University (Voronezh, Russian Federation)

https://orcid.org/0000-0002-5222-0756

tomina-e-v@yandex.ru

Received August 8, 2025; approved after reviewing October 3, 2025; accepted for publication October 15, 2025; published online April 01, 2026.